Electronic Supplementary Information

For

Molecular Engineering of Polyoxometalate-Porphyrin Ion-Pair Hybrids: Crystallographic Insight and Visible-Light Driven Photocatalytic Oxidative Coupling of Amines

Rohith Phaneendra Bandaru,[a,#] Asmita Dileep Gaonkar,[b,#] Kiran Vankayala,[b,] Bharat Kumar Tripuramallu [a,*]*

a. Dr. LARA Centre for Energy Materials, Department of Chemistry, Vignan's Foundation for Science Technology and Research (Deemed to be University), Vadlamudi, Guntur-522 213, Andhra Pradesh, India, Email: aryanbharat@gmail.com, drbkt_sh@vignan.ac.in

b. Functional Materials for Electrochemistry and Solar Energy (FunMatES) group, Energy and Environmental Chemistry Lab, Department of Chemistry, Birla Institute of Technology and Science, Pilani, K. K. Birla Goa Campus, NH 17B Bypass Road, Zuarinagar, Goa 403726, India. E-mail: kiranv@goa.bits-pilani.ac.in, kiran2cu@gmail.com

# Both authors contributed equally

Contents:

1. Chemicals: Pyrrole (Sigma, 99%), 4-Pyridine carboxaldehyde (TCI, 99.5%), Iodo methane (Sigma, 99%), Sodium molybdate dihydrate (Sigma, 99%), tetrabutylammonium bromide (Sigma, 99%), Triethanolamine (Loba Chemie), $AgNO_3$ (Loba Chemie, 99.9%), t-butyl alcohol (Qualigens, 99.5%), 1,4-Diazabicyclo[2.2.2]Octane (Molychem, 99%), p-benzoquinone (Loba, 98%), Benzylamine (Sigma, 99%), N-benzylidene benzylamine (Sigma, 99%), Dodecane (TCI, 99.5%), o-Tolidine (Alfa Aesar, 98%) Acetonitrile (Qualigens, 99.8%). All the chemicals were procured from commercial suppliers and used without further purification.

2. Characterization

Powder XRD patterns were obtained using an X-ray Diffractometer (Bruker D8 Advance) with Cu-Kα radiation (λ = 1.5405 Å). The Raman spectra were obtained using Lab RAM, HR Horiba France with an excitation wavelength of 532 nm. The UV-visible diffuse reflectance spectra (UV-vis DRS) were recorded using a UV-visible Jasco V770 spectrometer with an integrated sphere setup and $BaSO_4$ as a reference. The morphology of the as-prepared samples was examined using a field emission scanning electron microscope (Quanta FEG250, FEI). Mott-Schottky (M-S) measurements were performed in three-electrode electrochemical cell using electrochemical workstation (Biologic SP150e). The standard calomel electrode (Hg/Hg_2Cl_2/Sat. KCl) (SCE) was used as reference electrode, ITO slide coated with POM-POR hybrid catalyst was used as working electrode and graphite rod was used as auxiliary electrode respectively. The electrolyte was used as 0.1 M Na_2SO_4 (pH = 6.9). The working electrode was prepared by drop-casting the dispersion of POM-POR onto pre-cleaned ITO slide. The slurry was made with 2 mg of catalyst dispersed in 500 µL of ethanol and 10 µL of Nafion. Further 200 µL was coated on the ITO slide.

3. Synthesis

3.1. Synthesis of tetrabutylammonium hexamolybdate $[Bu_4N]_2[Mo_6O_{19}]$

$$6Na_2MoO_4 + 10HCl + 2(n\text{-}C_4H_9)_4NBr \longrightarrow [(nC_4H_9)_4N]_2[Mo_6O_{19}] + 10NaCl$$

Sodium molybdate dihydrate (1.25 g) was dissolved in 5 mL of distilled water and acidified with 3.0 mL of 6.0 N HCl in a 100.0 mL round-bottom flask. To this acidic solution, a solution of tetrabutylammonium bromide (1.21 g in 2.0 mL water) was added dropwise under continuous stirring, resulting in the formation of a white precipitate. The reaction mixture was then heated to 75-80 °C and stirred for 45 minutes, during which the precipitate gradually turned yellow. The resulting crude solid was collected by filtration, washed with distilled water, and dissolved in acetonitrile. The solution was cooled to 20 °C and allowed to stand for 24 hours to facilitate crystallization. The yellow crystalline product was collected by suction filtration, washed twice with 20 mL of diethyl ether, and dried under vacuum to yield tetrabutylammonium hexamolybdate. IR (KBr pellet, cm^{-1}): 2960 (m), 2930 (m), 2870 (m), 1480 (m), 1460 (m), 1380 (w), 960 (s, ν(Mo=O)), 870 (s, ν(Mo–O–Mo)), 760 (m, ν(Mo–O)), 720 (w), 650 (w).

3.2. Synthesis of *meso*-tetra(4-pyridyl) porphyrin (H_2TPP)

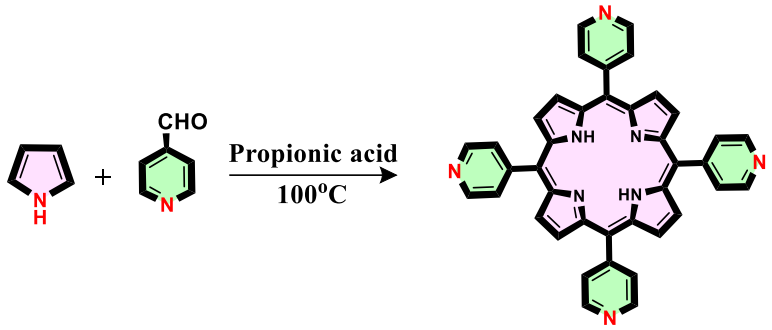

Scheme S1. Scheme representing the synthesis of tetrapyridyl porphyrin. (**H_2TPP**)

meso-Tetra(4-pyridyl)porphyrin (H_2TPP) was synthesized using a slightly modified procedure based on the Adler–Longo method. In a typical reaction, 3.76 mL (0.04 mol) of 4-pyridinecarboxaldehyde and 2.80 mL (0.04 mol) of freshly distilled pyrrole were introduced into 150 mL of propionic acid under a nitrogen atmosphere with vigorous stirring. The reaction mixture was maintained under reflux for approximately 40 minutes to promote the formation of the porphyrin macrocycle. After cooling to room temperature, the reaction was quenched with 150 mL of deionized water, and the product was extracted using dichloromethane 150 mL. The combined organic layers were dried over anhydrous sodium sulphate, and the solvent was removed under reduced pressure. The crude product was purified by sequential washing with dimethylformamide (DMF) and methanol to eliminate unreacted residues. The final product was obtained as a dark purple powder in 20% yield. Molecular formula: $C_{40}H_{26}N_8$. Molecular weight: 618.70. Elemental analysis calcd. (%) for $C_{40}H_{26}N_8$: C, 77.65; H, 4.24; N, 18.11 and found C, 77.52; H, 4.18; N, 18.24. ^{1}H-NMR ($CDCl_3$) (ppm): 8.2 (d, 8H, *m*-pyridyl), 8.87 (s, 8H, pyrrole), 9.0 (d, 8H, *o*-pyridyl), -2.97 (s, 2H, NH).

3.3. Synthesis of Tetrakis N-methyl pyridyl porphyrin [H_2TPPMe_4] I_4

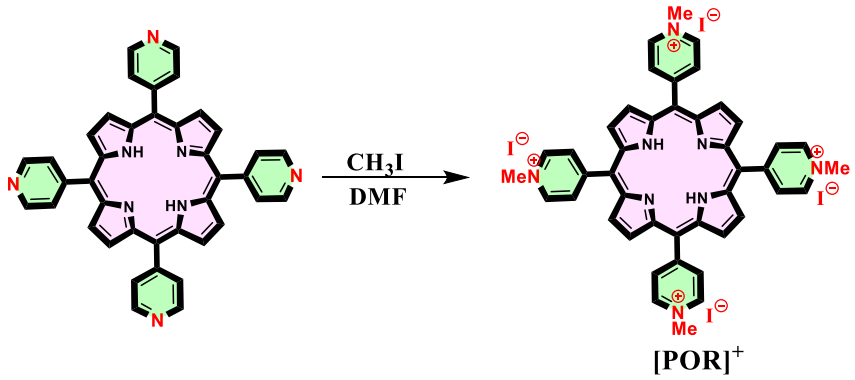

Scheme S2. Scheme representing the methylation of tetrapyridyl porphyrin.

An excess of iodomethane (4 mL, 64.3 mmol) was added to a suspension of 5,10,15,20-tetrakis(4-pyridyl)porphyrin (100 mg, 162 µmol) in anhydrous dimethylformamide (DMF, 20 mL). The reaction

mixture was stirred in a sealed vessel at 40 °C for 5 hours to ensure complete methylation of the pyridyl nitrogen atoms. After cooling to room temperature, the reaction mixture was treated with diethyl ether to induce precipitation of the product. The resulting solid was collected by filtration and washed thoroughly with diethyl ether to remove residual reagents. The crude precipitate was redispersed in a 1:1 mixture of acetone and water, and the solvent was removed under reduced pressure. Upon reprecipitation, the methylated porphyrin product was filtered, washed with acetone, and dried under vacuum to yield a reddish-brown solid. Molecular formula: $C_{44}H_{38}N_8I_4$. Molecular weight: 1186.48. Elemental analysis calcd. (%) for $C_{44}H_{38}N_8I_4$: C, 44.54; H, 3.23; N, 9.44 and found C, 44.62; H, 3.18; N, 9.24. ^{1}H-NMR (DMSO$_{d6}$) (ppm): 9.5 (d, 8H, *m*-pyridyl), 9.2 (s, 8H, pyrrole), 9.0 (d, 8H, *o*-pyridyl), 4.7 (s, 12 H, methyl), -3.1 (s, 2H, NH).

3.4. Synthesis of POM-POR hybrid material $[H_2TPPMe_4][Mo_6O_{19}]_2 \cdot 4DMF$

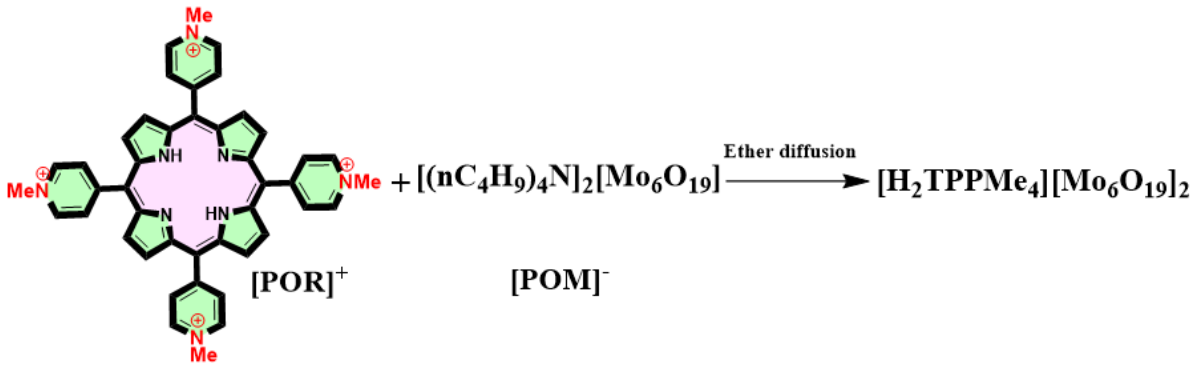

Scheme S3. Scheme representing the synthesis of POM-POR scaffold.

Tetrabutylammonium hexamolybdate (1.0 mmol) was dissolved in 2 mL of acetonitrile and gently heated until clear. Separately, tetrakis(N-methylpyridinium-4-yl)porphyrin (1.0 mmol) was dissolved in 2 mL of DMF and added to the molybdate solution, yielding a precipitate that was filtered. For crystallization, the solid was dissolved in DMF and placed in an inner vial within a 10 mL screw-capped vial containing diethyl ether to enable slow vapor diffusion. After three weeks, crystals formed, which were collected, washed with diethyl ether, and dried under vacuum for characterization. Molecular formula: $C_{56}H_{68}N_{12}O_{42}Mo_{12}$. Molecular weight: 2732.60. Elemental analysis calcd. (%) for $C_{56}H_{68}N_{12}O_{42}Mo_{12}$: C, 24.61; H, 2.51; N, 6.15 and found C, 24.72; H, 2.68; N, 6.24. ^{1}H-NMR (DMSO$_{d6}$) (ppm): 9.5 (d, 8H, *m*-pyridyl), 9.2 (s, 8H, pyrrole), 9.0 (d, 8H, *o*-pyridyl), 4.7 (s, 12 H, methyl).

[1]H NMR spectra of precursors and POM-POR.

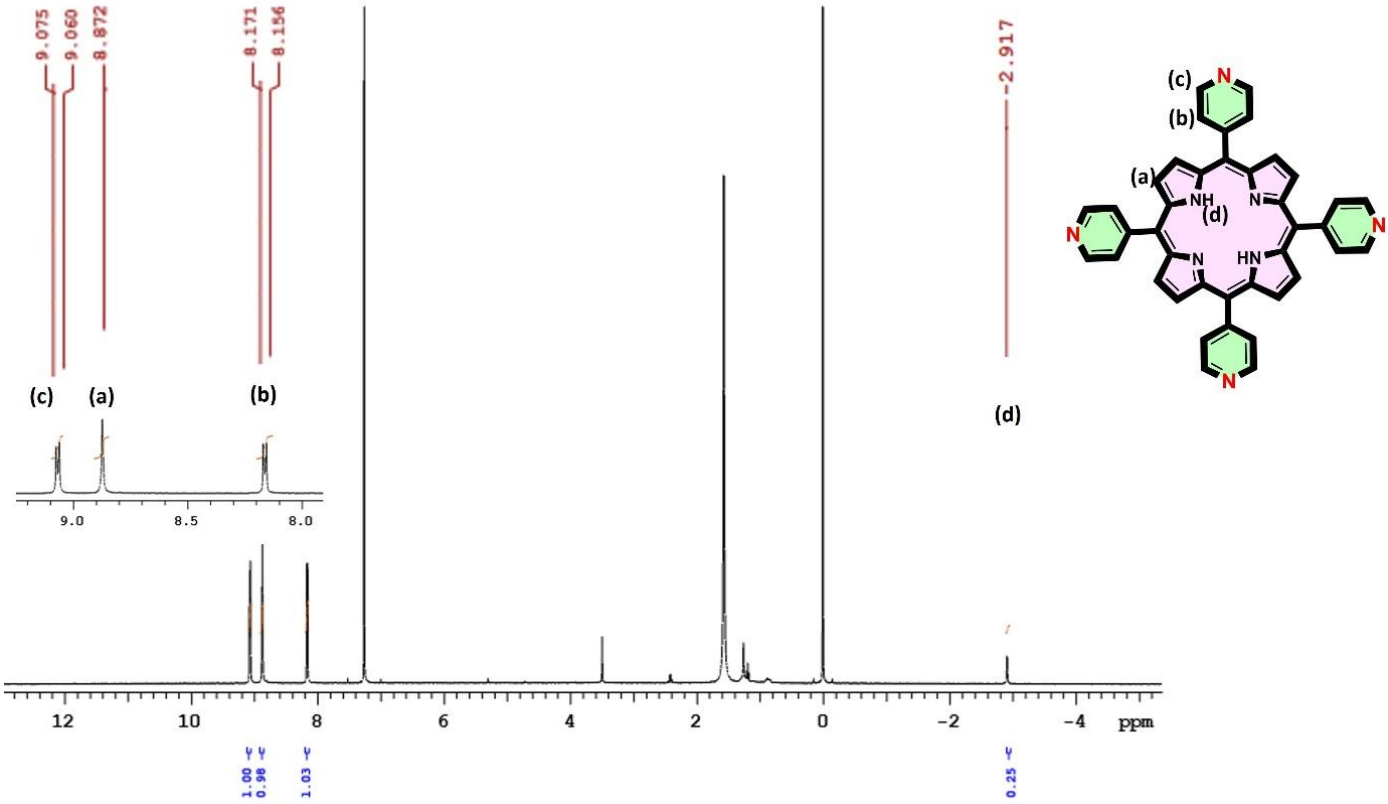

Fig.S1 [1]H NMR spectra of Tetrapyridyl porphyrin ($CDCl_3$, 400MHz).

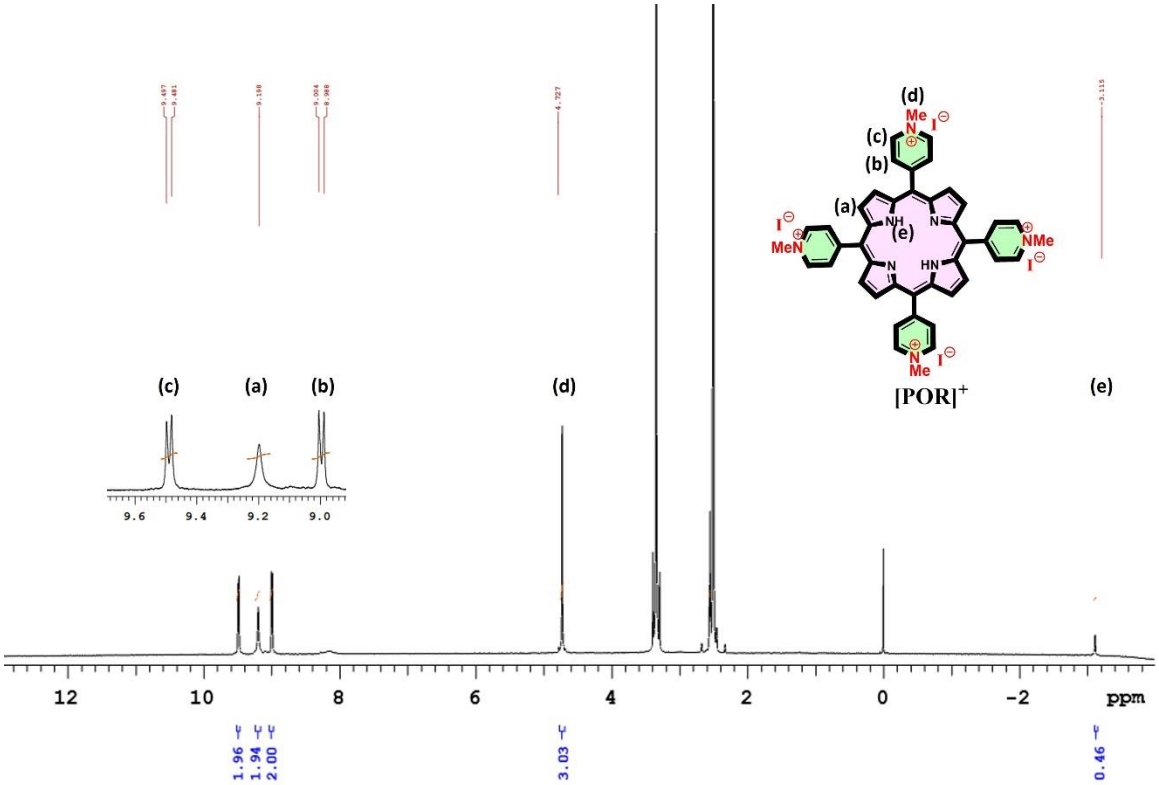

Fig.S2. ^{1}H NMR spectra of N-methyl Tetrapyridyl porphyrin(POR) (DMSO-d_6, 400MHz).

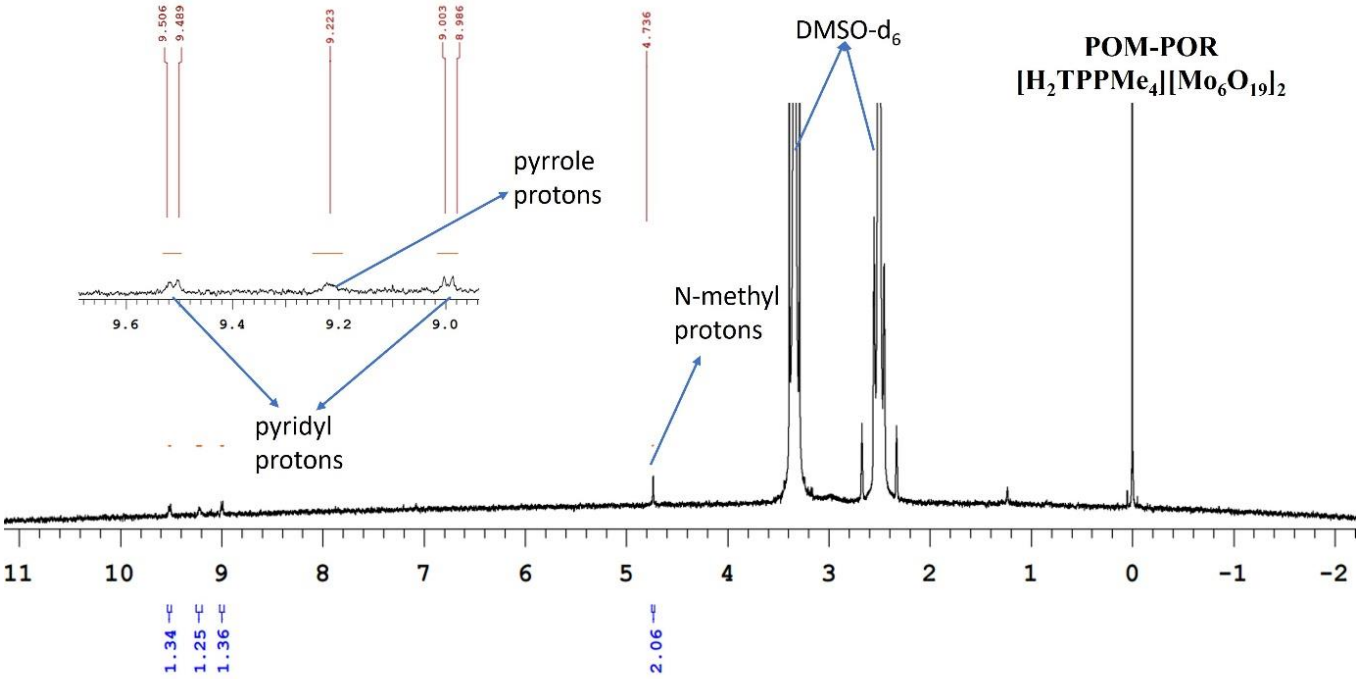

Fig.S3. ^{1}H NMR spectra of POM-POR (DMSO-d_6, 400MHz).

4. FT-IR studies

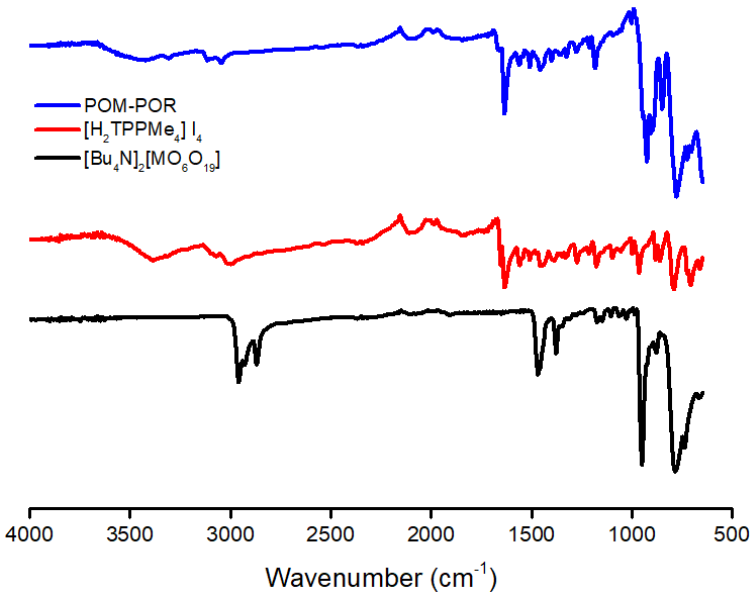

Fig.S4. FTIR spectra of POM-POR, POR and POM respectively.

As shown in Fig. S4, the FTIR spectra displayed characteristic Mo–O stretching vibrations between 950–780 cm^{-1}, confirming the presence of the polyoxometalate (POM) framework. The porphyrin (POR) exhibited distinct C=C and C–N stretching bands in the 1600–1400 cm^{-1} region. In the FTIR spectrum of hybrid, the appearance of both POM and POR features clearly validated the successful formation of the POM–POR hybrid.

5. TGA analysis

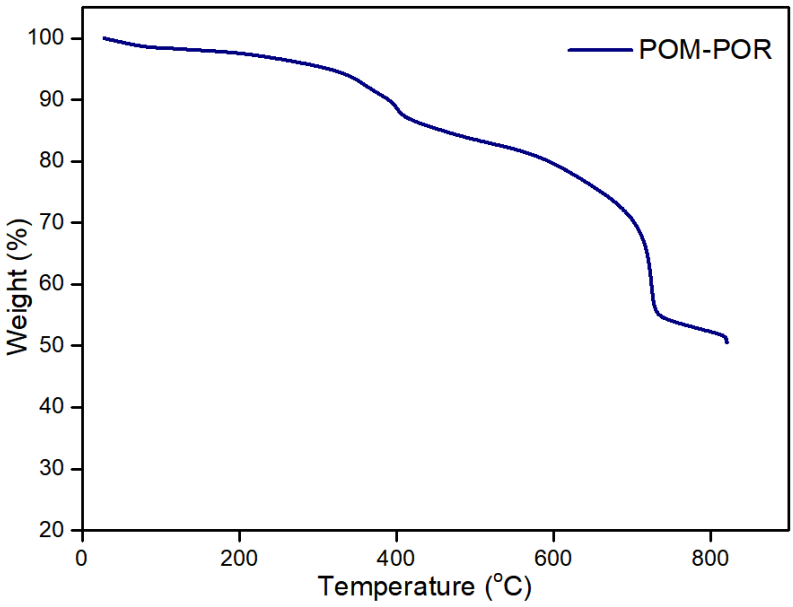

Fig.S5. TGA curve of POM-POR hybrid carried out under N_2 atmosphere at a heating rate of 20 °C min^{-1}

Thermogravimetric analysis (TGA) of the POM–POR hybrid was carried out using an STA-7200 instrument under a nitrogen atmosphere with a heating rate of 20 °C min^{-1} from room temperature to 800 °C. The TGA profile reveals an initial weight loss of approximately 13% up to 405 °C, attributed to the release of five coordinated DMF molecules present in the crystal lattice. A subsequent 33% weight loss between 405 °C and 730 °C corresponds to the thermal decomposition of the porphyrin moiety. The remaining 55% residue beyond 730 °C represents the thermally stable metal oxide derived from the POM unit.

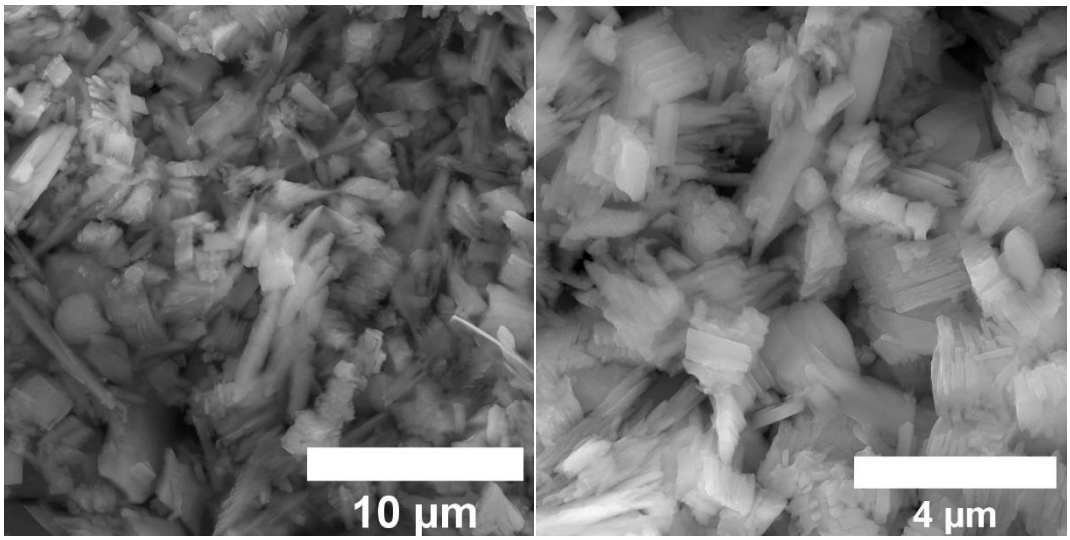

Fig. S6. FESEM image of POM-POR hybrid recorded at different magnifications.

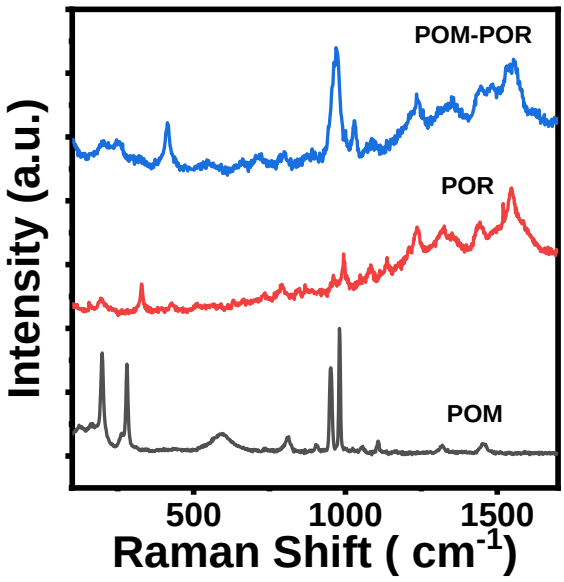

Fig. S7. Raman spectra of POM, POR and POM-POR hybrid recorded using 532 nm laser.

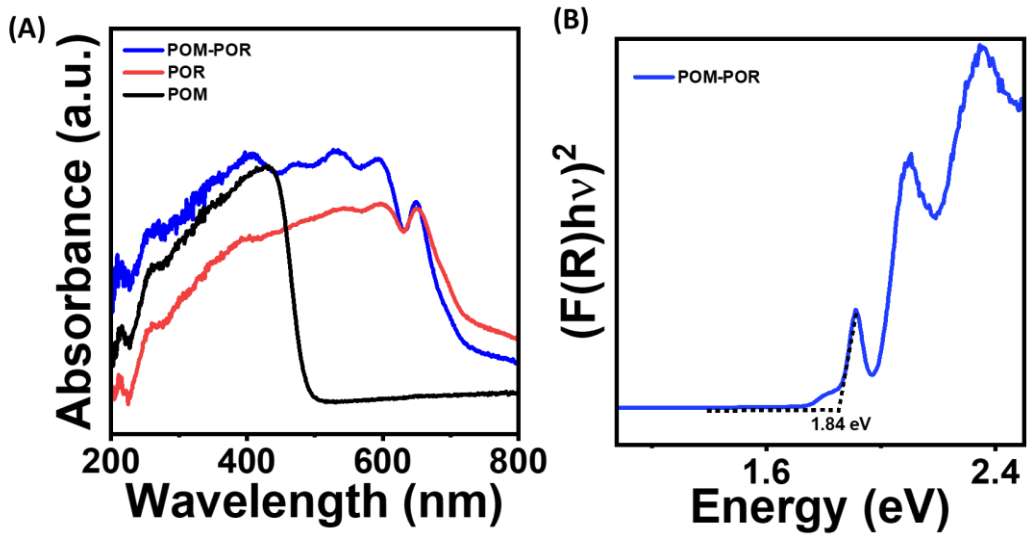

Fig. S8. (A) UV-Vis DRS of POM, POR and POM-POR hybrid and (B) Tauc plot of POM-POR hybrid.

6. Single crystal X-ray diffraction measurement

The X-ray measurements [Bruker-Apex Duo diffractometer, IμS micro-focus MoKα radiation] were carried out at ca. 110(2) K on crystal coated with a thin layer of amorphous oil. These structure were solved by direct and Fourier methods and refined by full-matrix least-squares (using standard crystallographic software (SHELXT-2014, SHELXL-2014).[1-2] The structure found to contain disordered crystallization solvent DMF. Some of the solvent content could not be reliably identified, and modeled by discrete atoms. Correspondingly, the contribution of the disordered solvent moieties was subtracted from the diffraction pattern by the SQUEEZE procedure and PLATON software.[3] Solvent accessible void space in the unit cell is 155 $Å^3$ with residual electron count of 39 electrons.

Crystallographic Table S1

CCDC No	2499082
Empirical formula	$C_{56}H_{66}Mo_{12}N_{12}O_{42}$
Moiety formula	$[H_2TPPMe_4][Mo_6O_{19}]_2{\cdot}4DMF$
Formula weight	2730.48
Temperature/K	296.15
Crystal system	triclinic
Space group	P-1
a/Å	11.4946(3)
b/Å	11.7114(3)
c/Å	17.2449(4)
α/°	83.4680(10)
β/°	72.0640(10)
γ/°	69.9960(10)
Volume/Å3	2075.31(9)
Z	1
ρcalcg/cm3	2.185
μ/mm-1	1.845
F(000)	1326.0
Crystal size/mm3	0.28 × 0.24 × 0.15
Radiation	MoKα (λ = 0.71073)
2Θ range for data collection/°	3.702 to 56.73
Index ranges	-15 ≤ h ≤ 14, -15 ≤ k ≤ 15, -23 ≤ l ≤ 23
Reflections collected	38481
Independent reflections	10351 [Rint = 0.0191, Rsigma = 0.0191]
Data/restraints/parameters	10351/0/554
Goodness-of-fit on F2	1.030
Final R indexes [I>=2σ (I)]	R1 = 0.0269, wR2 = 0.0636
Final R indexes [all data]	R1 = 0.0300, wR2 = 0.0653
Largest diff. peak/hole / e Å-3	2.64/-1.00

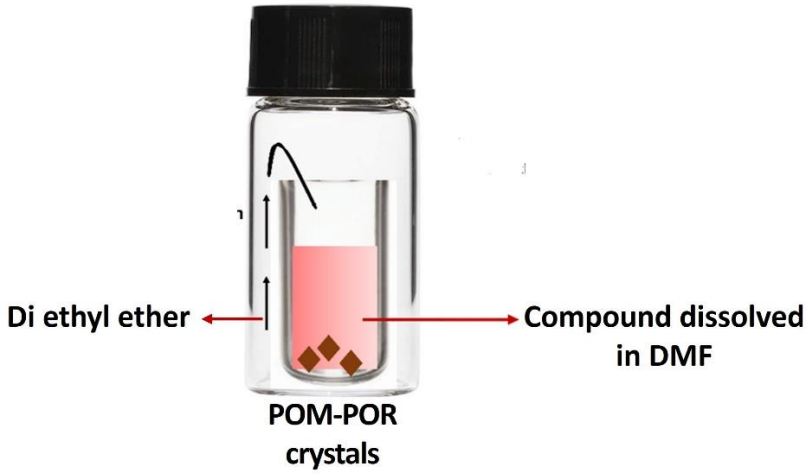

Fig. S9. Vapour diffusion method followed to grow single crystals of POM-POR hybrid using diethyl ether.

7. Additional illustrations of crystal structure

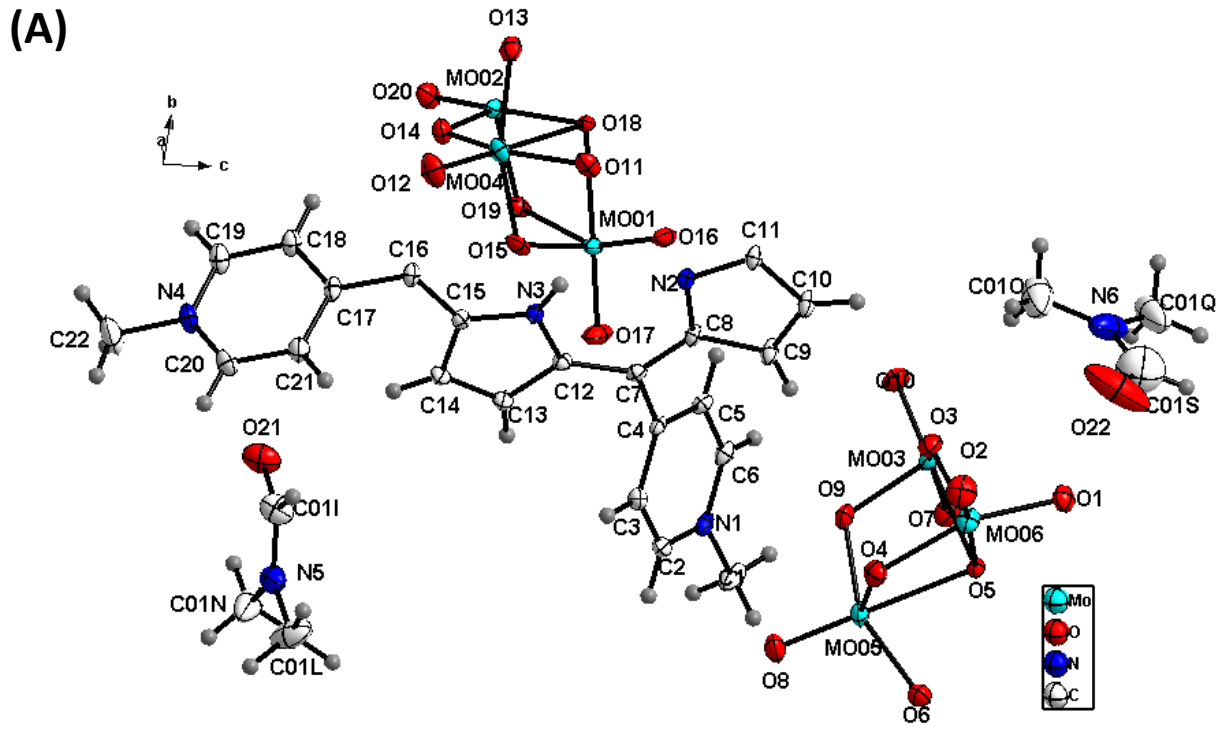

Fig. S10A. An ORTEP diagram of the POM-POR hybrid crystal with thermal ellipsoids drawn at the 50 % probability level is shown.

Hirshfeld surface analyses

Hirshfeld surface analysis was carried out using CrystalExplorer 21.5 to investigate close intermolecular contacts between neighbouring molecules and to generate the corresponding two-dimensional (2D) fingerprint plots for visualizing these interactions. The refined crystallographic information file (.cif) was used as the input, and the analysis was performed to the N-methylated porphyrin unit to visualize the interactions experienced by the porphyrin unit in the polyoxometalate matrix. The normalized contact distance (d_{norm}) is calculated using the van der Waals radii of the atoms and is displayed as a color-coded surface (Fig i). In this representation, red regions indicate close contacts. The shape index and curvedness parameters reveal how molecules pack together, especially when they adopt planar stacking patterns (Fig. S10 (ii & iii).

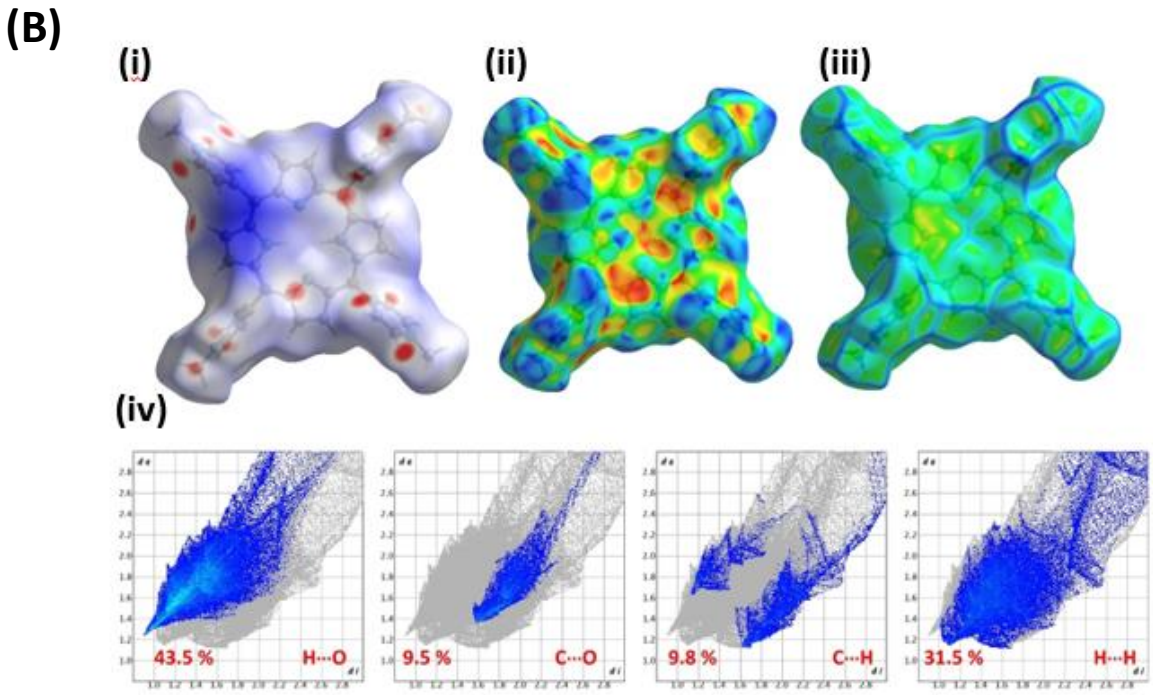

Fig. S10B. Hirshfeld surface analysis of the N-methylated porphyrin unit, (i) d_{norm} surface (ii) Shape index surface (iii) Curvedness surface and (iv) The two-dimensional fingerprint plots.

As displayed in figure a, several red spots on the surface of the porphyrin macrocycle clearly indicates closest contacts which leads to tight packing of the porphyrins in the POM matrix, more particularly around meso positions of the porphyrin macrocycle. The two-dimensional (2D) Hirshfeld fingerprint plots (iv) indicates nearly 43.5% of interactions are dominated by $C\text{-}H_{(POR)}\cdots O_{(POM)}$ contacts between C-H groups of porphyrin to oxygen atoms in $Mo_6O_{19}^{2-}$. While the $C_{(POR)}\cdots O_{(POM)}$ distribution (9.5%) and the C···H contacts (9.8%) due to interaction between porphyrin macrocycle and solvent DMF contributes to the crystal packing. Together, these contributions show that C-H···O interactions are the principal stabilizing force, supported by abundant $C_{(POR)}\cdots O_{(POM)}$ contacts and C-based interactions that collectively reinforce the three-dimensional crystal architecture.

8. Photocatalytic studies

8.1. Photocatalytic oxidation of Benzylamine amine (BzAM) to *N*-benzylidenebenzylamine (BzIM)

The aerobic oxidative coupling of BzAM under photochemical conditions was performed in a custom-designed 15 mL quartz reactor using various photocatalysts such as Polyoxometalates (POM), Porphyrin (POR) and Polyoxometalate-Porphyrin (POM-POR) hybrid. Typically, 4 mg of photocatalyst was suspended in 10 mL of acetonitrile (ACN) containing 20 mM of BzAM. Prior to photocatalysis, the reaction mixture was sonicated for 10 min., followed by purging the reactor with high-pure O_2 gas for 15 min. A custom-built white LED was used as a light source. The photoreactor was kept 4 cm away from the light source. The temperature of the reactor was maintained using a water bath. The products formed during the course of photocatalytic oxidation were monitored using Gas Chromatography (GC) (Agilent 8890) equipped with a Flame Ionization Detector (FID) and HP-5 capillary column (30 m × 0.32 mm, 0.25 μm). The carrier gas used was N_2 with a flow rate of 5 mL/min. The inlet and the detector temperature were kept at 250 °C. Initially, the column temperature was held at 100 °C for 3 min., subsequently ramped to 200 °C at a ramp rate of 12 °C/min. Aliquot (500 μL) of the reaction mixtures collected from the reactor after illumination was filtered through a 0.45 μm nylon syringe filter to separate photocatalyst particles from the reaction mixture. Subsequently, 2 μL of the reaction mixture containing Dodecane (2 mM) that acted as internal standard, was injected into GC. The calibration plots were obtained using standard solutions of different concentrations of BzAM and N-benzylidenebenzylamine (BzIM). The concentration of the product formed during photocatalytic oxidation was determined from the calibration plot. The selectivity (%), conversion (%) and yield (%) were calculated using the following equations;[4]

$$\text{Selectivity}\ (\%) = (2 \times C_{BzIM}/C_0 - C_{BzAM}) \times 100 \quad (1)$$

$$\text{Conversion}\ (\%) = (C_0 - C_{BzAM}/C_0) \times 100 \quad (2)$$

$$\text{Yield}\ (\%) = (2 \times C_{BzIM}/C_0) \times 100 \quad (3)$$

where C_o is the initial concentration of BzAM, C_{BzAM} is the concentration of the remaining BzAM after a particular time of reaction and C_{BzIM} is the concentration of BzIM formed after a specific time of the photocatalytic reaction.

To investigate the active species involved in the photocatalytic oxidation process, experiments were performed by adding various scavengers such as p-benzoquinone (BQ), 1,4-Diazabicyclo[2.2.2]octane (DABCO), $AgNO_3$, triethanolamine (TEOA) and tert-butyl alcohol (t-BuOH) into the reaction mixture as these are known to scavenge superoxide radical ($O_2^{-\bullet}$), singlet oxygen ($^1O_2$), electrons (e^-), holes (h^+) and hydroxyl radicals (•OH) respectively.

Hot filtration test was performed to validate the robustness of the POM-POR catalyst. After 10 min. of the reaction, the POM-POR catalyst was separated from the reaction mixture by filtration and the reaction mixture was further subjected to illumination.

8.2. Identification of H_2O_2

The formation of H_2O_2 during photocatalytic oxidation of BzAM was determined using spectrophotometric method with O-tolidine as probe. The reaction mixture collected before and after 20 min. of illumination was separated from catalyst particles via filtration using 0.45 μm syringe filter. A 1.5 mL aliquot of this was mixed with 0.5 mL of O-tolidine (1% tolidine in 0.1 M HCl) and the mixture was kept in dark for 10 min. prior to recording absorption spectra.[5]

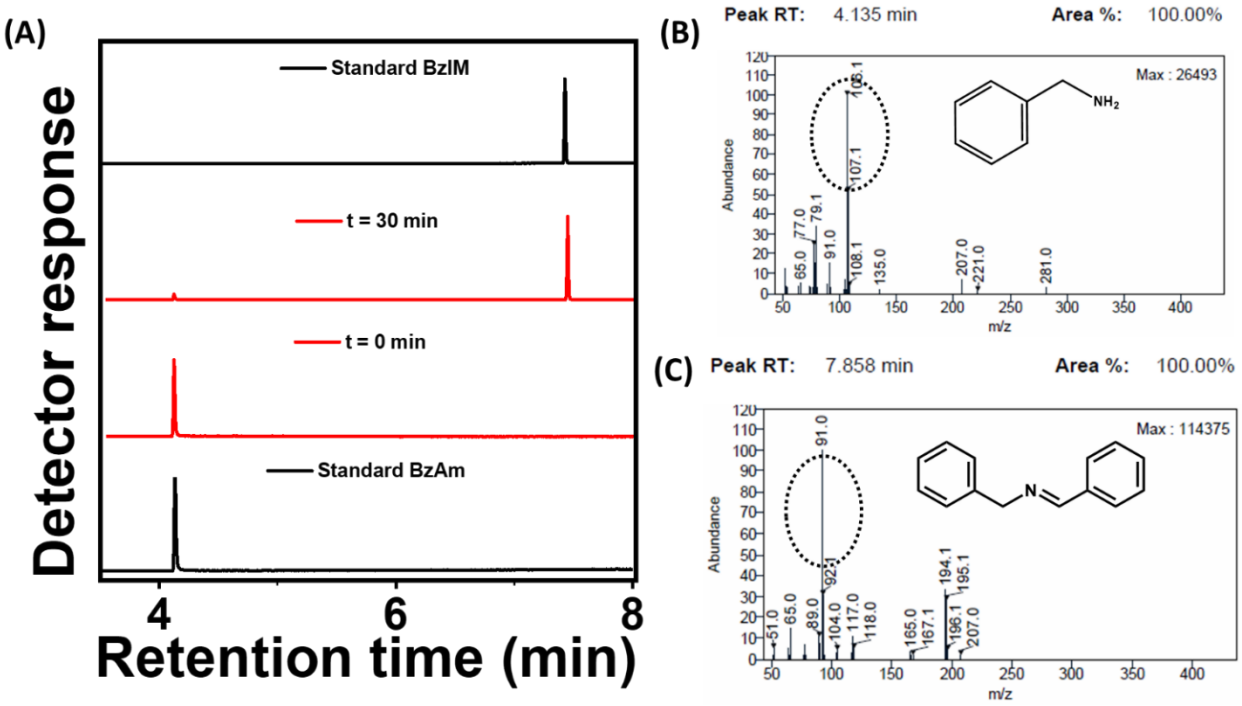

Fig. S11. (A) GC-MS chromatograms obtained for the reaction mixture when time of illumination t = 0 min and t = 30 min. Reaction conditions: 4 mg POM-POR, 10 mL of acetonitrile (ACN) containing 20 mM Benzylamine (BzAM). The chromatograms of standard 20 mM BzAM and 10 mM benzylidenebenzylamine (BzIM) are also shown in (A). (B) & (C) represent the mass spectra corresponding to the standard BzAM and BzIM.

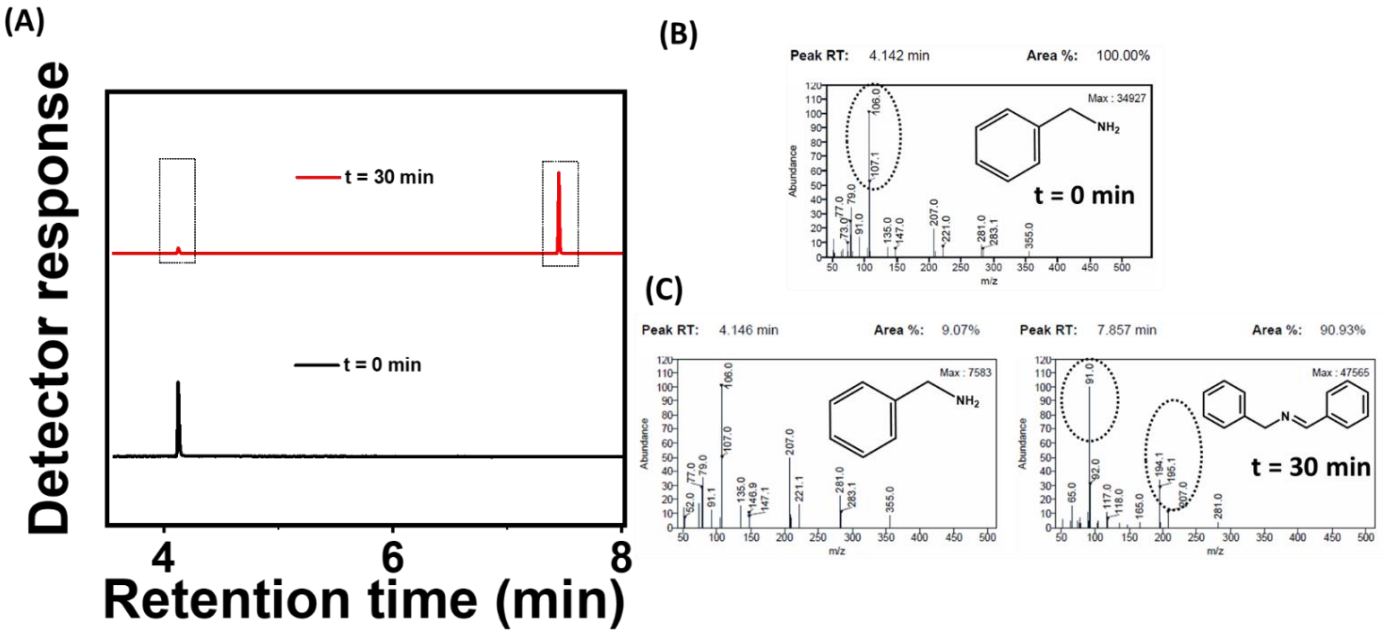

Fig. S12. (A) GC-MS chromatograms obtained for the reaction mixture when time of illumination t = 0 min and t = 30 min. Reaction conditions: 4 mg POM-POR, 10 mL of acetonitrile (ACN) containing 20 mM BzAM. (B) and (C) represent the mass spectra corresponding to the eluent collected at Rt = 4.15 min. for t =0 sample and eluent collected at Rt = 4.15 min. & 7.85 min. for t = 30 min. respectively.

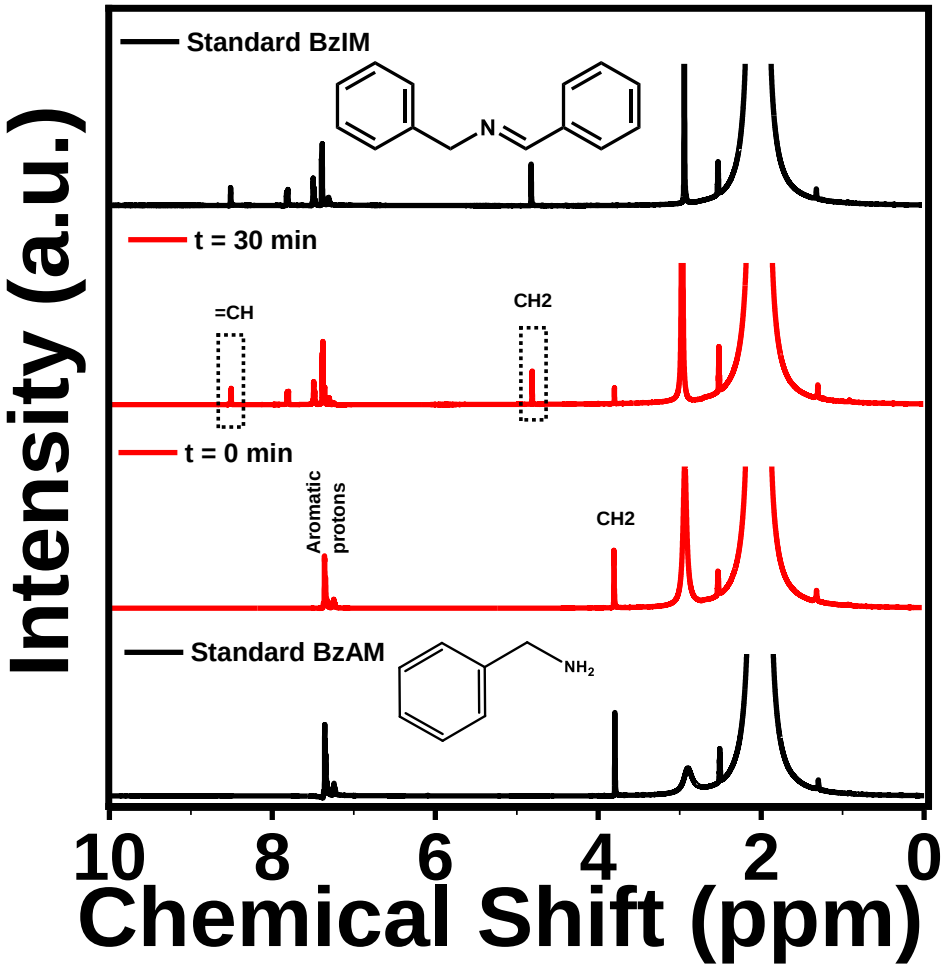

Fig. S13. ^{1}H NMR spectra obtained for the reaction mixture collected before (t=0 min.) and after illumination (t=30 min.). The ^{1}H NMR spectra of standard 20 mM benzylamine (BzAM) and 10 mM Benzylidenebenzylamine (BzIM) are also shown in the figure.

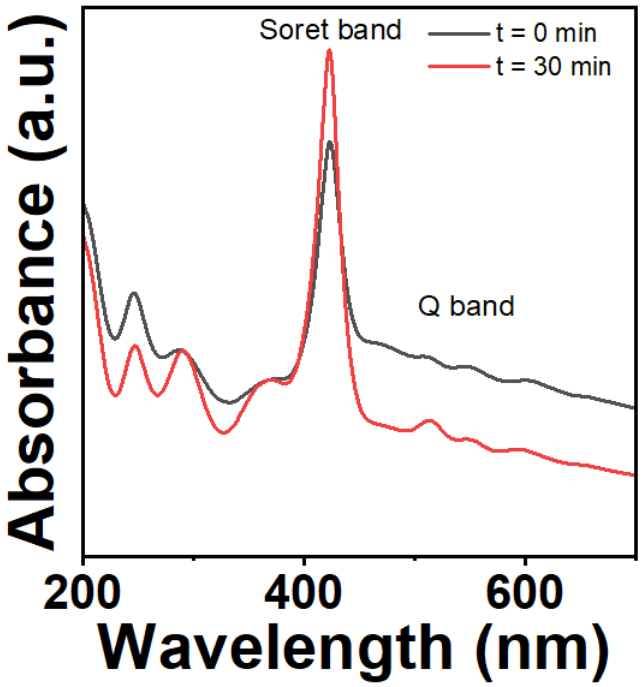

Fig. S14. UV-visible absorption of reaction mixture collected before and after illumination with light. Reaction condition: 4 mg POM-POR, 10 mL Acetonitrile, purged with oxygen and light illuminated for 30 min. The 1 mL aliquot was taken and diluted to 1 mL acetonitrile to record UV-visible spectra.

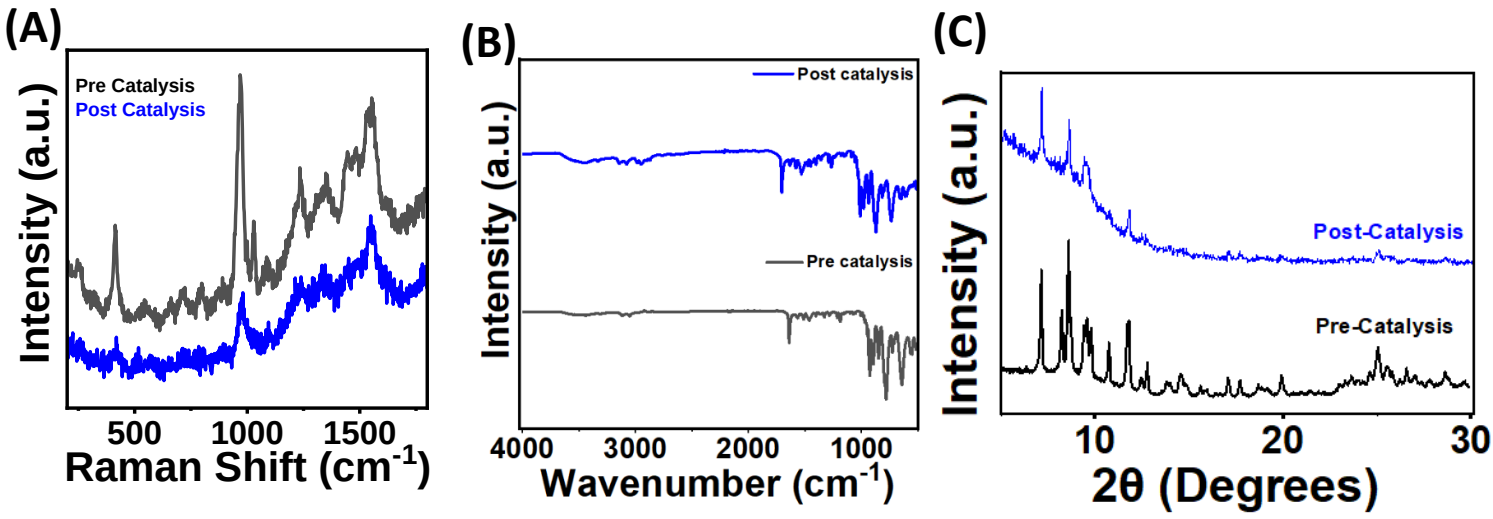

Fig. S15(A) Raman spectra, (B) FTIR spectrac and (C) XRD patterns recorded for POM-POR before and after photocatalysis.

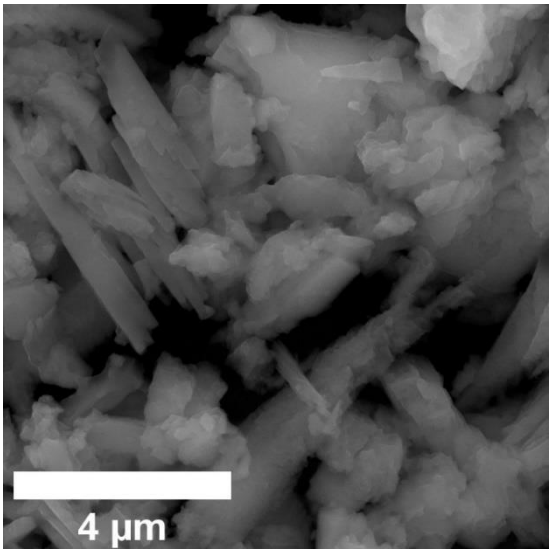

Fig. S16. FESEM image of POM-POR hybrid catalyst recovered after 5 runs of photocatalysis.

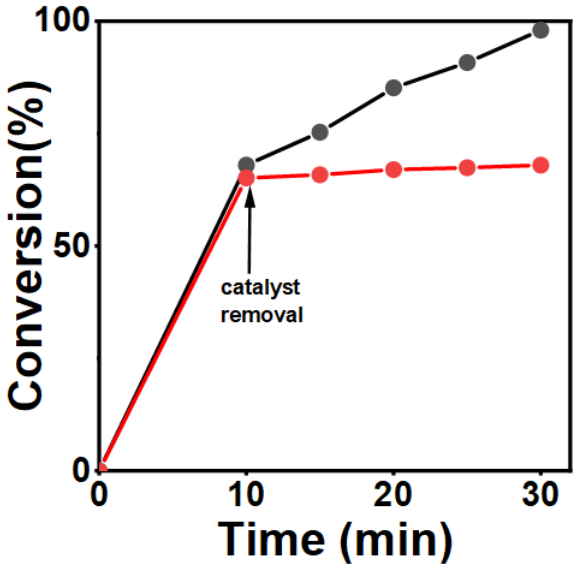

Fig.S17. Hot filtration test of POM-POR in the photocatalytic oxidation of BzAM.

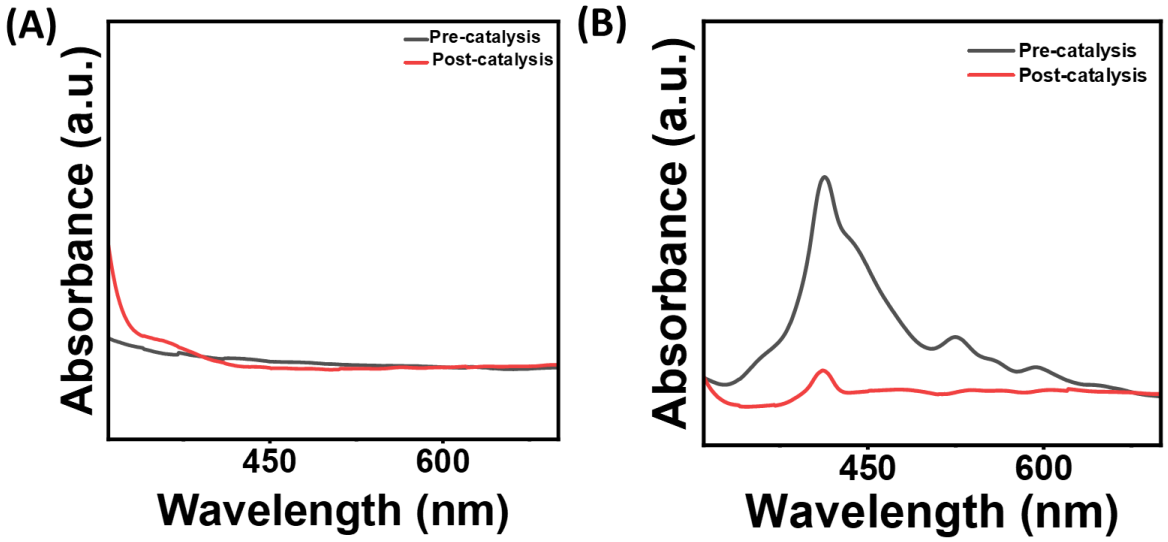

Fig. S18. UV-visible absorption of reaction mixture collected before and after illumination with light, when catalyst used was (A) POM-POR hybrid and (B) POR (TPP). Reaction condition: 4 mg catalyst (POM-POR or POR), 20 mM BzAM in 10 mL acetonitrile, purged with oxygen. 100 μL of the reaction mixture (filtrate) collected after photocatalysis and diluted to 2 mL acetonitrile.

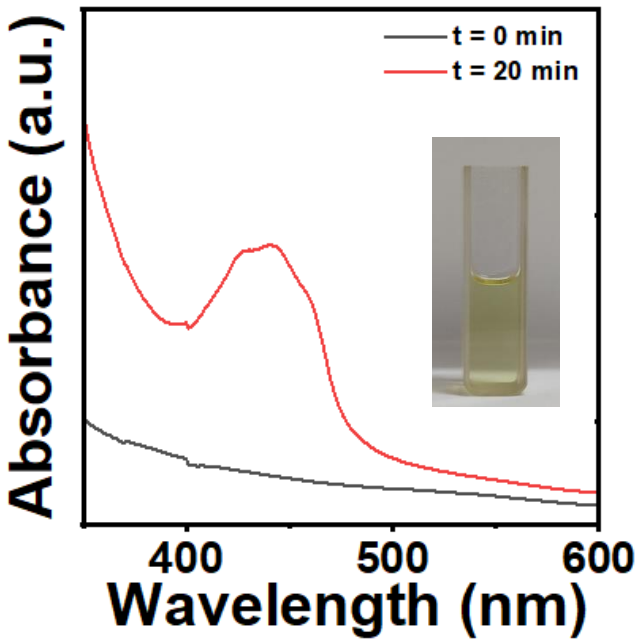

Fig. S19. Spectrophotometric qualitative determination of the formation of H_2O_2 in the reaction mixture during photocatalytic oxidation using O-Tolidine solution. Reaction condition: 4 mg POM-POR, 20 mM of BzAM in 10 mL O_2- saturated acetonitrile. Inset shows the cuvette consisting of yellow colored solution due to the reaction of H_2O_2 formed in photocatalysis with O-tolidine.

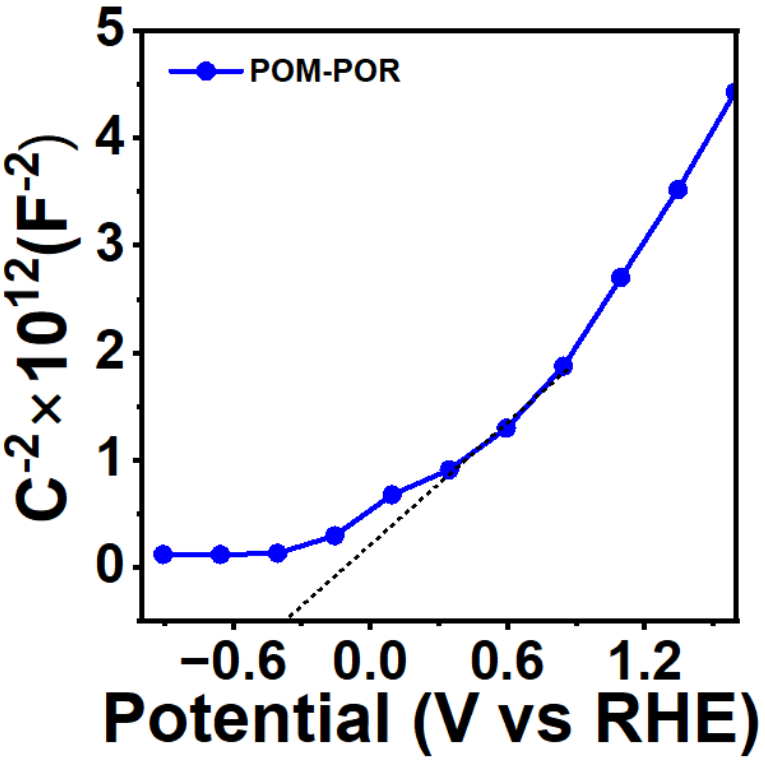

Fig. S20. Mott-Schottky plot of POM-POR hybrid obtained in 0.1 M Na_2SO_4 (pH= 6.9) at 1000 Hz.

Table S2: Comparison of the photocatalytic activities of POM and POR-based systems for the production of BzAM to BzIM reported in the literature.

S. No	Photocatalyst	Amount of Catalyst	Conc. of substrate	Time	Light source	TOF (h^{-1})	Sel. (%)	Conv. (%)	Yield (%)	Reference (DOI)
1	$H_2TPP+TBA_4H_4[SiW_{10}O_{36}]$ (Porphyrin)	0.003 mol%	2.5 µmol	10 min	Xe lamp, 400 nm	-	-	-	99	10.1021/jacs.3c11394
2	$Ru(bpy)_3[Mo_6O_{19}]$-(POM)	0.6mmol %	0.4 mmol	25 min	10 W 445 nm LED	392	98	>99	98	10.1021/acs.inorgchem.2c01243
3	$Na_{13}K_{2.5}H_{6.5}[Ru_4(H_2O)_2(Cl)_2(WO_2)_4(AsW_9O_{33})4]\cdot_{43}H_2O$-(POM)	0.1mol%	1 mmol	24 h	10 W COB LED	20	-		97	10.1021/acs.inorgchem.2c00718
4	$(NH_4)_{41}H_7[K_3(H_2O)_3(P_2W_{15}Ta_3O_{62})_6(Mo_2O_4CH_3CO_2)_3(MoO_3)_2]\cdot 85H_2O$ (1 mol %)-(POM)	1 mol %	0.2 mmol	24 h	300 W Xe lamp	4	100	96	96	10.1021/acsami.9b16694
5	$TBA_6[\{Ce(H2O)\}2\{Ce(CH_3CN)\}^{2-}$ (μ^4-O)(γ-$SiW_{10}O_{36})_2]$ (1 mol %) -(POM)	1 mol%	0.2 mmol	24 h	Visible light	4	-		96	10.1002/anie.201403215
6	$\{[Zn(HPYI)_3]_2(DPNDI)\}[BW_{12}O_{40}]^{2-}$	10 mg	5 mmol	16 h	10 W white LED	223	-		99	10.1016/j.jcat.2019.06.040
7	$K_6H[\{Ru_2Cl(H_2O)(CH_3COO)_2\}\{WO(H_2O)\}_2(PW_9O_{34})_2]\cdot 14H_2O$	0.1mol%	1 mmol	24 h	Visible light (λ > 400 nm	41	-		97	10.1021/acs.inorgchem.1c03282
8	NaRh-SiW_{12} (POM)	0.5mol%	1 mmol	12 h	10W white LED	120	-		96.1	10.1021/acs.inorgchem.3c01749
9	POM-POR	20 mg	20 mM (0.2 mmol)	30 min	White LED	175	100	99	100	**This Work**

Table S3: Photocatalytic oxidation of different amines into imines using POM-POR catalyst. Reaction conditions: 10 mg of POM-POR catalyst, 20 mM of substrate in 10 mL ACN, purged with oxygen and light is illuminated for 30 min.

Entry	Substrate	Reactant	Conversion (%)
1	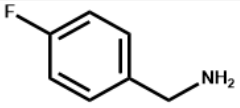	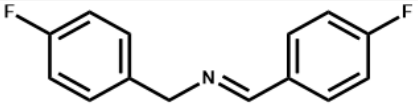	94 %
2	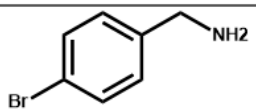	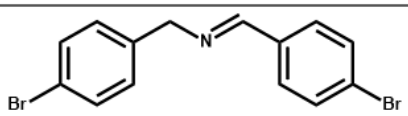	86.3 %
3	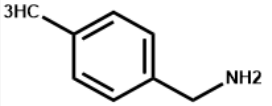	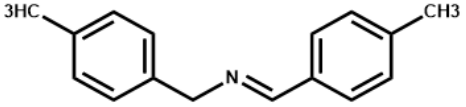	99.4 %
4	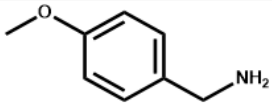	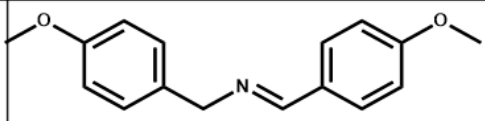	99.6%
5	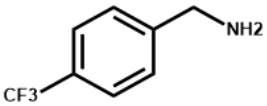	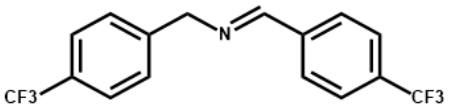	75.7%
6	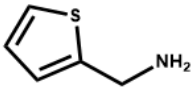	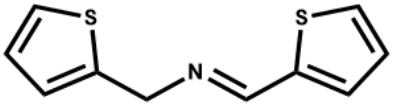	65%

References

1. G. M. Sheldrick, *Acta Crystallogr. A Found. Adv.*, 2015, **71**, 3–8.
2. G. M. Sheldrick, *Acta Crystallogr. C Struct. Chem.*, 2015, **71**, 3–8
3. A. L. Spek, *Acta Crystallogr. C Struct. Chem.*, 2015, **71**, 9–18
4. J. Kou, C. Lu, J. Wang, Y. Chen, Z. Xu and R. S. Varma, *Chem. Rev.*, 2017, **117**, 1445–1514.
5. J. Liu, Y. Zhang, L. Lu, G. Wu and W. Chen, *Chem. Commun. (Camb.)*, 2012, **48**, 8826–8828.